

Supplementary Information for

**SILVER ION REDUCTION IN NON-AQUEOUS LIQUID OLIGOMERS
WITH TERMINAL EPOXY AND AMINO GROUPS
FOR *IN SITU* SYNTHESIS OF SILVER NANOPARTICLES**

Ivan N. Senchikhin^{1,*}, Petr V. Konarev², Vladimir V. Volkov²,
Alena P. Ryazanova³, Elena S. Zhavoronok³

¹ – *A.N. Frumkin Institute of Physical Chemistry and Electrochemistry,
Russian Academy of Sciences, 31, Bldg. 4, Leninsky prospect, Moscow 119071, Russia*

² – *A.V. Shubnikov Institute of Crystallography, Kurchatov Complex of Crystallography and
Photonics, National Research Centre “Kurchatov Institute,” 59, Leninskiy prospect, Moscow
119333, Russia*

³ – *MIREA – Russian Technological University, Lomonosov Institute of Fine Chemical
Technologies, 86, prospect Vernadskogo, Moscow 119571, Russia*

*e-mail: isenchikhin@phyche.ac.ru

Contents

1. UV-vis spectra of epoxy resins and oligoamine with precursor	
Figure S1. Evolution of the wavelength values corresponding to the maximum of the absorption peak of UV-vis spectra of epoxy resins and oligoamine with precursor	3
Figure S2. Kinetic dependences of intensity of absorption bands at the peak maximum of UV-vis spectra of epoxy resins and oligoamine with precursor	4
2. DLS and SAXS raw data and processing results	
Figure S3. Dependences $\alpha(\tau)$ in the coordinates of a – zero, b – first and c – second order on the example of sample No. 4	5
Figure S4. Evolution of autocorrelation functions obtained in the DLS experiment	6
Figure S5. Evolution of the scattering curves obtained in the SAXS experiment	7
Figure S6. Typical size scattering intensity distributions (a) and particle number (b), obtained using the DLS	8
Figure S7. Evolution of diameters D_{10} , D_{50} and D_{90} , as well as SPAN, on synthesis time, according to DLS (a) and SAXS (b) methods, for system No. 4 (Table 2)	9
Figure S8. Theoretical SAXS scattering curves obtained for silver crystallites of sphere and cubic shapes.	10
Table S1. χ^2 values for SAXS data plotted in Fig. 4	11
3. UV-vis spectra of silver nitrate solution	
Figure S9. UV-vis spectra of a 2.9 wt.% silver nitrate solution	12

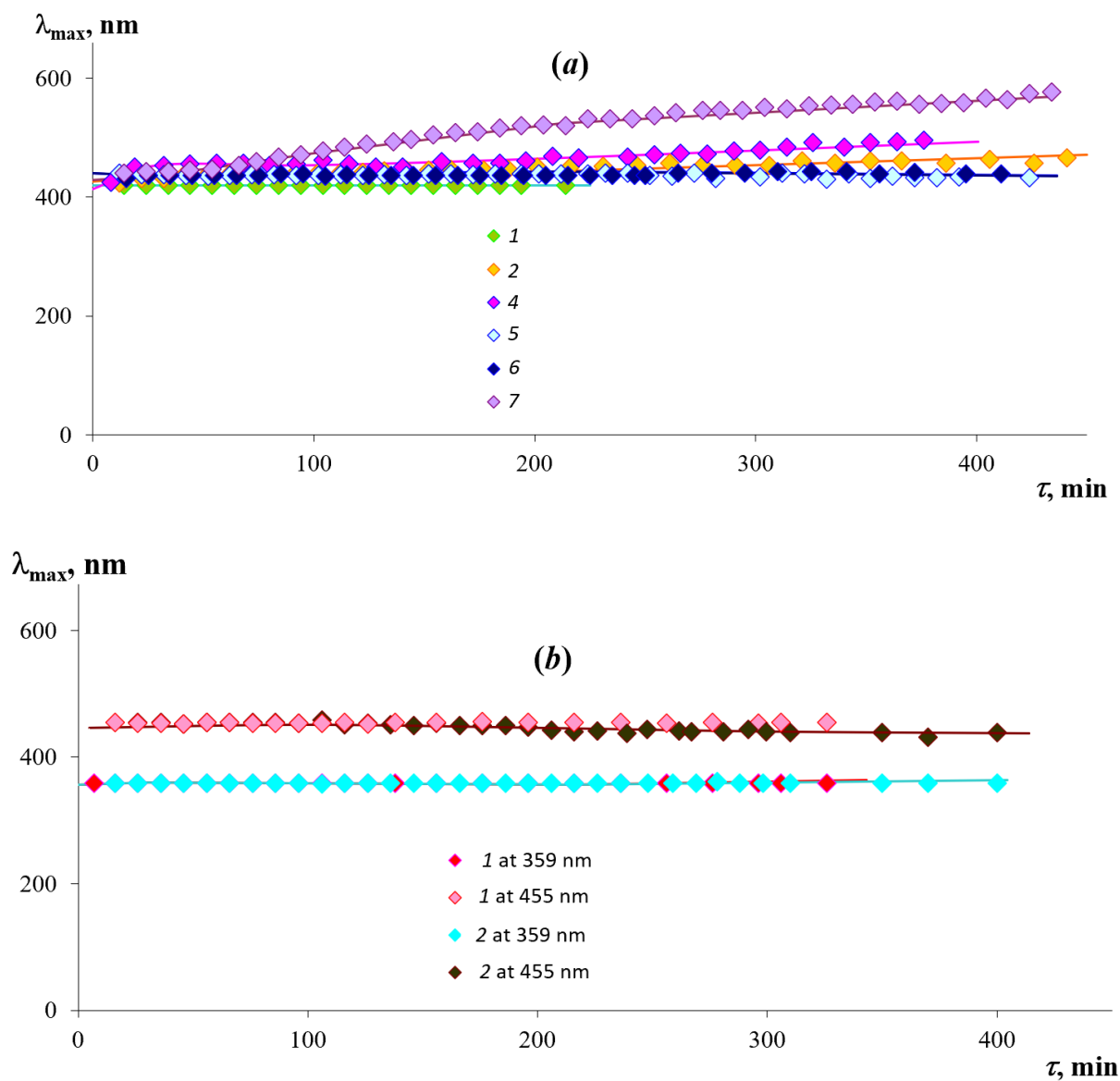


Figure S1. Evolution of the wavelength values corresponding to the maximum of the absorption peak of UV-vis spectra of epoxy resins (a) and oligoamine (b) with precursor. Row numbers in (a) correspond to the samples in Table 2. Row numbers in (b) correspond to the precursor concentration of 0.6 (1) and 0.3 (2) g/ 100 g of oligoamine at the acetonitrile content of 1.6 (1) and 2.8 g/ 100 g (2) of oligoamine, respectively

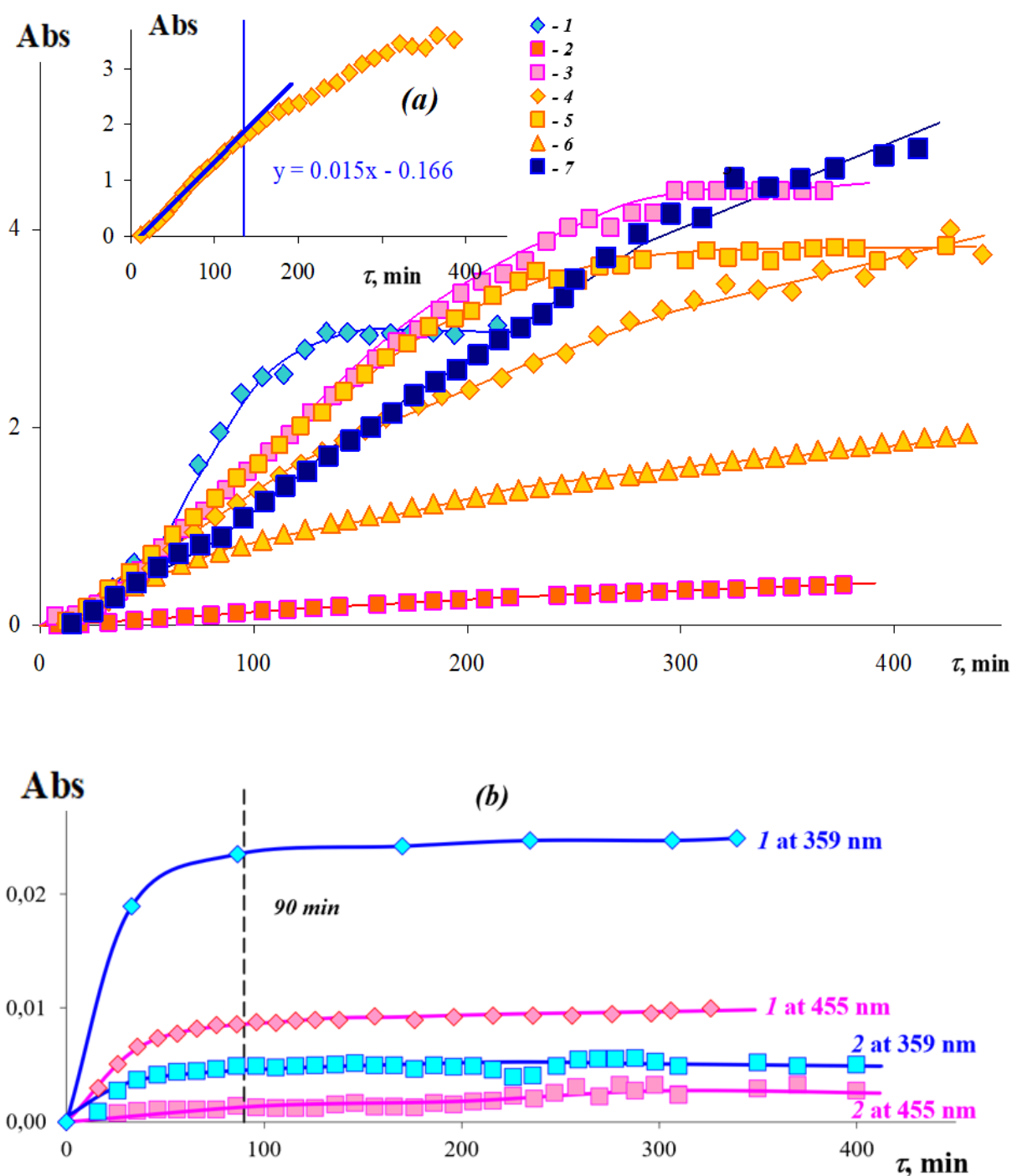


Figure S2. Kinetic dependences of intensity of absorption bands at the peak maximum of UV-vis spectra of epoxy resins (a) and oligoamine (b) with precursor. Row numbers in (a) correspond to the samples in Table 2. Row numbers in (b) correspond to the precursor concentration of 0.6 (1) and 0.3 (2) g/ 100 g of oligoamine at the acetonitrile content of 1.6 (1) and 2.8 g/ 100 g (2) of oligoamine, respectively

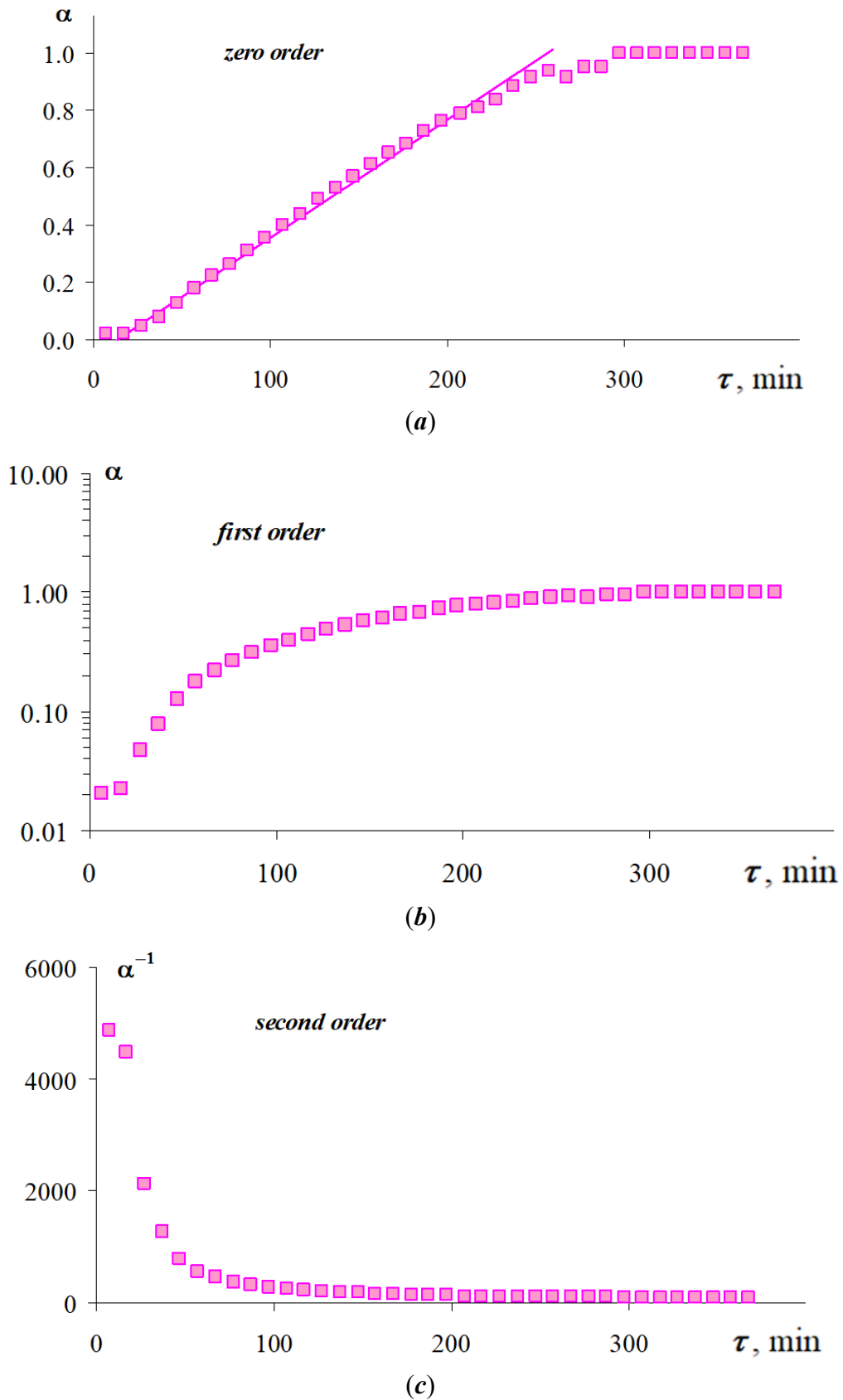


Figure S3. Dependences $\alpha(\tau)$ in the coordinates of **a** – zero, **b** – first and **c** – second order on the example of sample No. 4

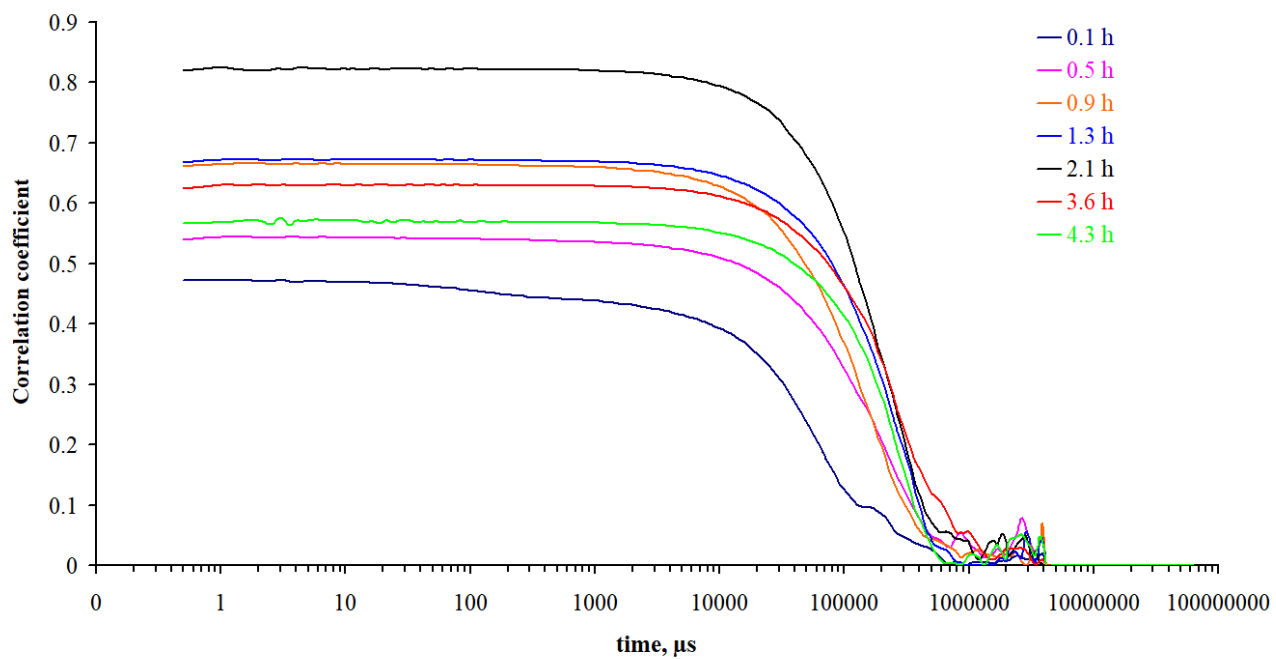
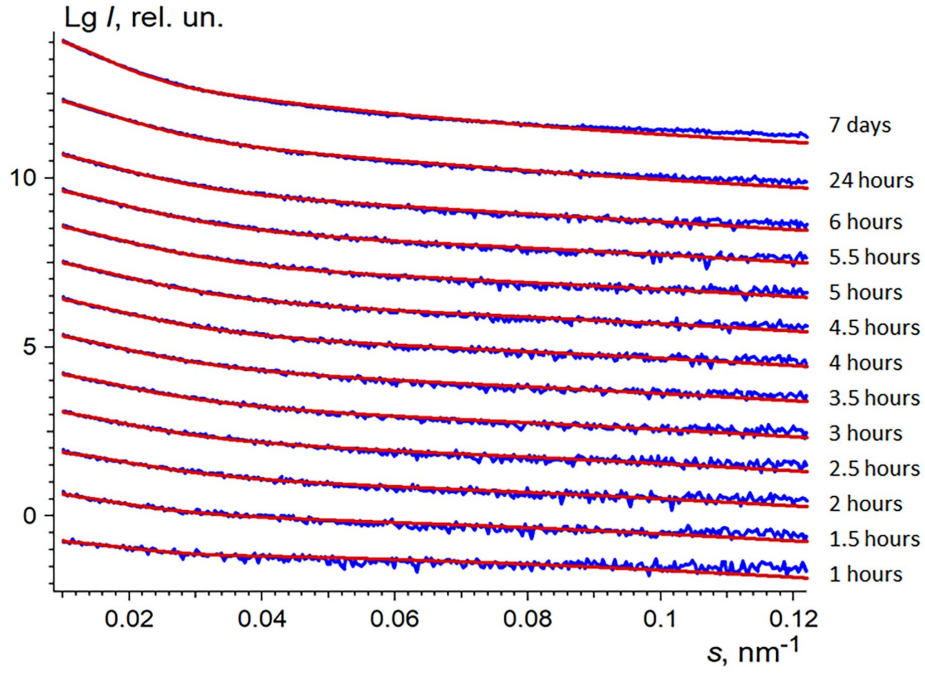
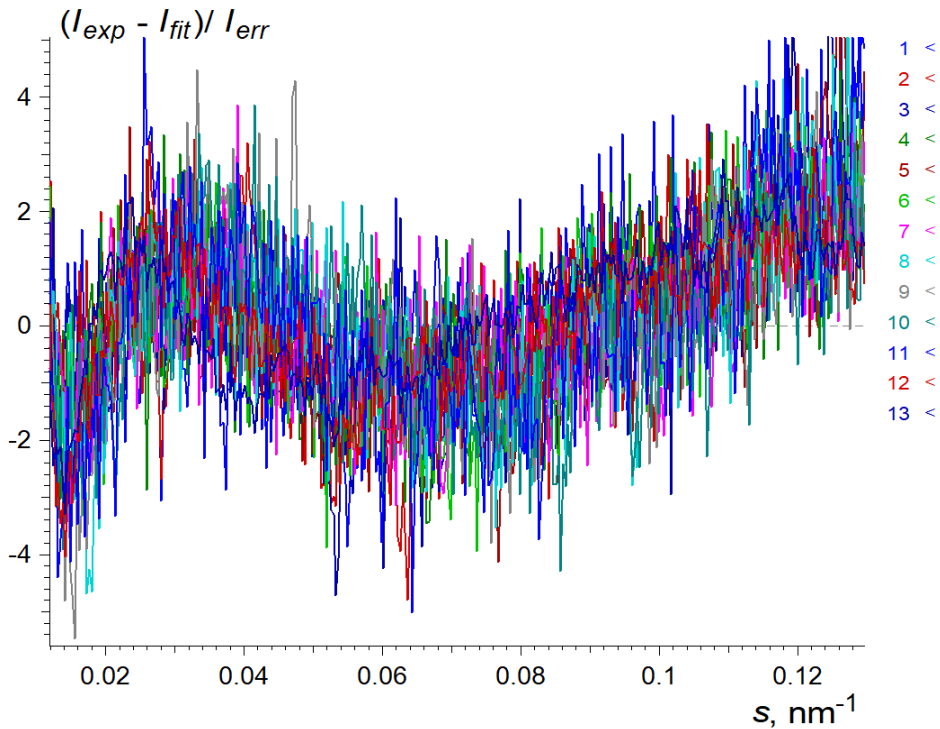


Figure S4. Evolution of autocorrelation functions obtained in the DLS experiment for system No.4 (Table 2)



(a)



(b)

Figure S5. (a) Evolution of the scattering curves obtained in the SAXS experiment for system #4 (Table 2). The blue curves show the experimental results and the red curves show the best approximations obtained by the MIXTURES program from the ATSAS package. The curves have been shifted relative to each other by one logarithmic order along the vertical axis to improve visualization;

(b) Residual plots depict the differences between experimental SAXS data (I_{exp}) and the best fits (I_{fit}), where I_{err} - error estimates of intensities, the curve numbering is ascending with time.

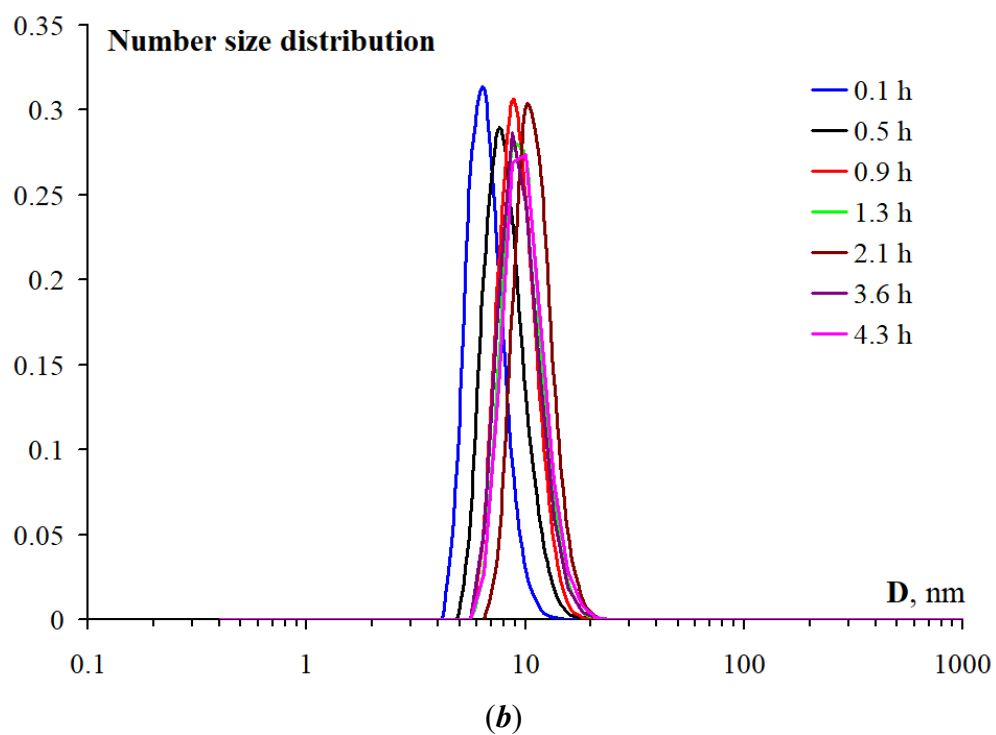
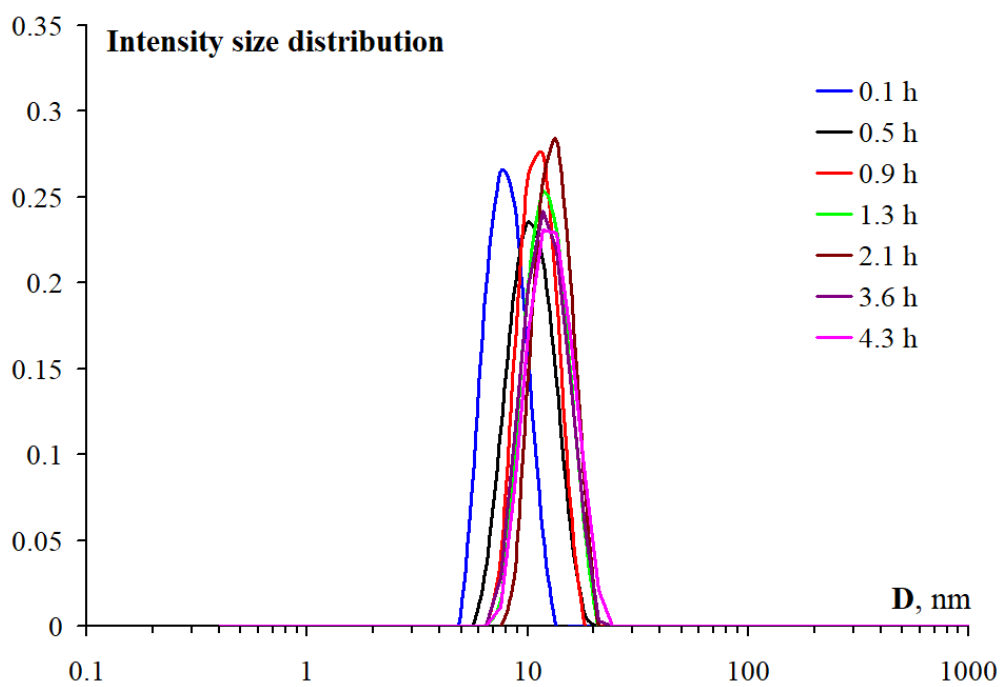


Figure S6. Typical scattering intensity (*a*) and particle number (*b*) size distributions, obtained using the DLS for system No. 4 (see Table 2)

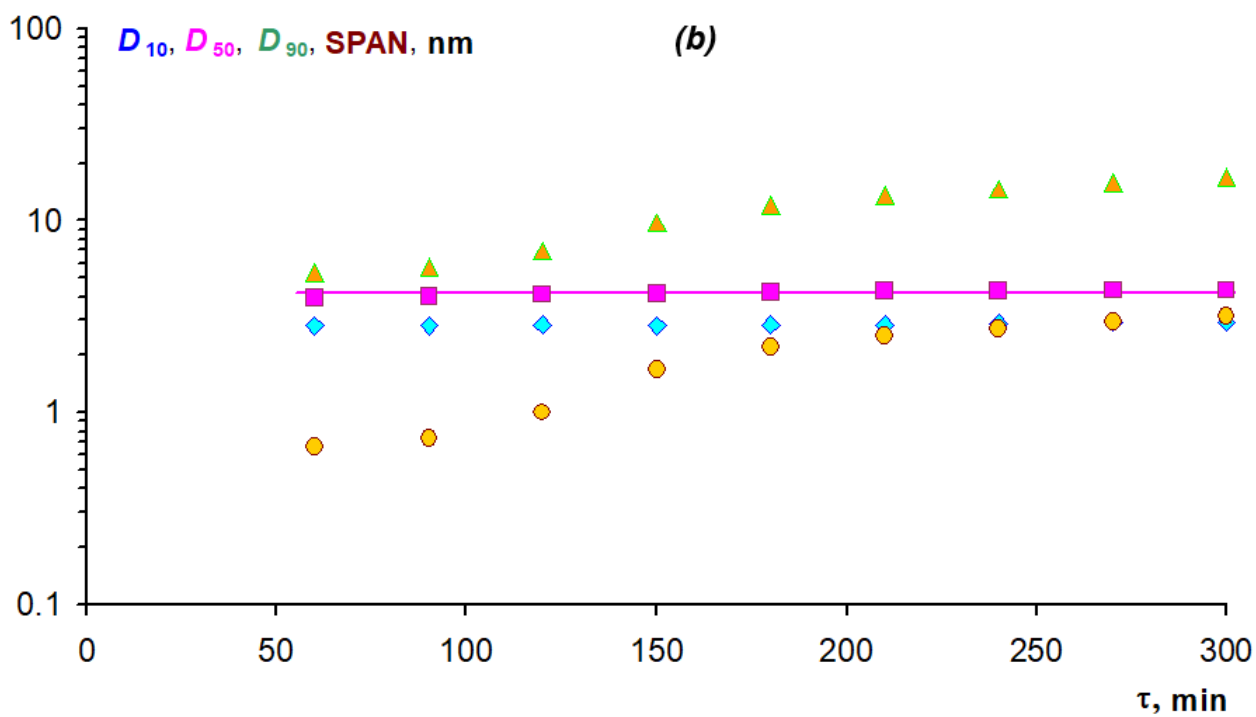
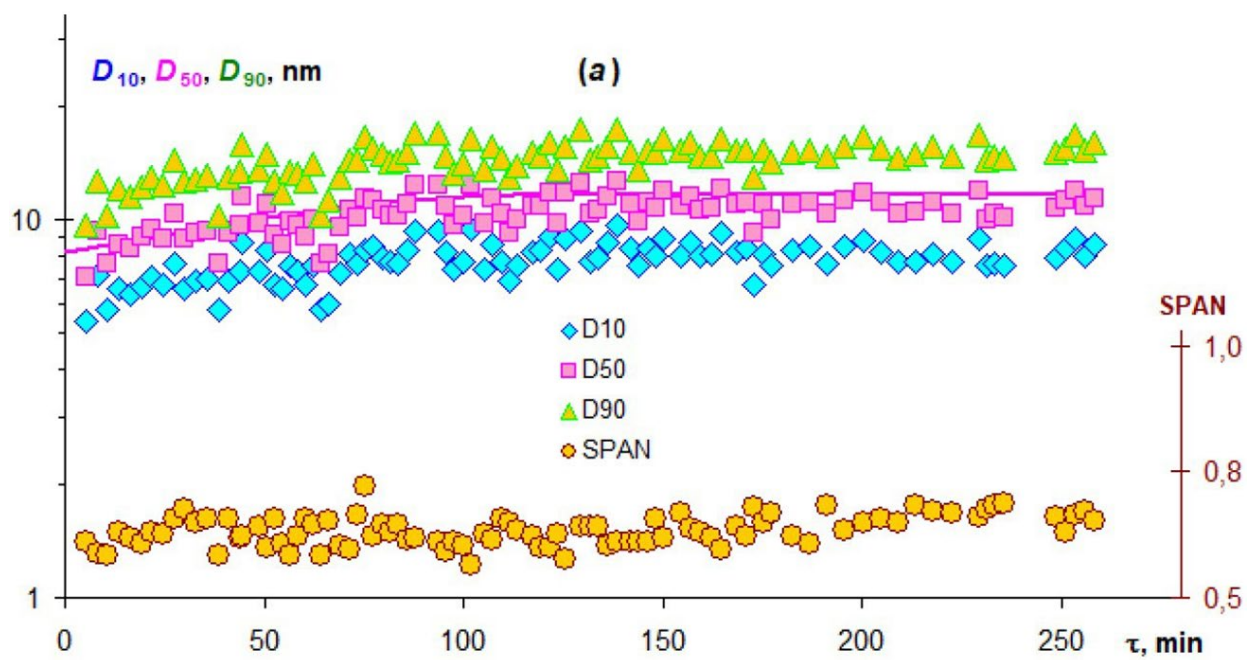


Figure S7. Evolution of diameters D_{10} , D_{50} and D_{90} , as well as SPAN, on synthesis time, according to DLS (a) and SAXS (b) methods, for system No. 4 (Table 2)

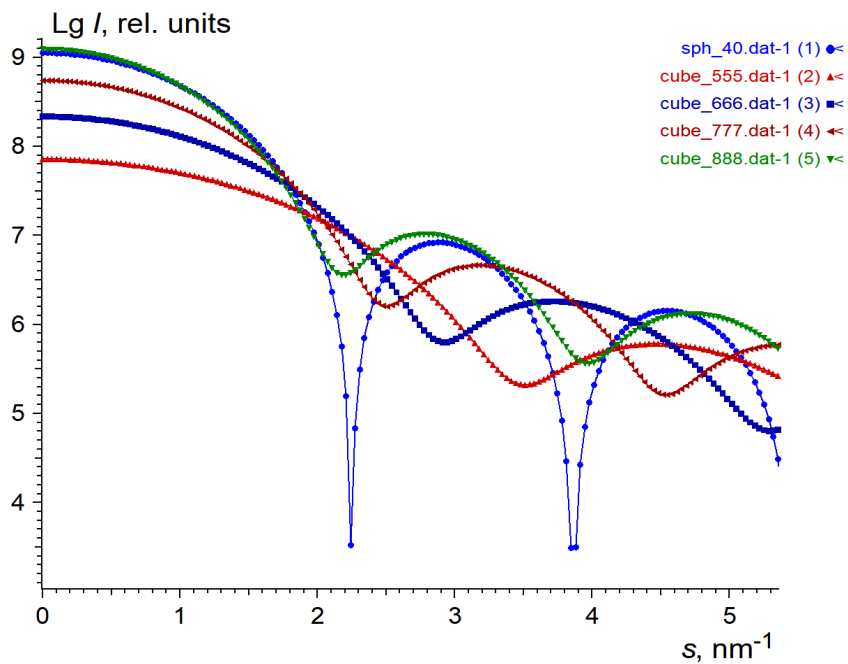


Figure S8. Theoretical scattering curves from: a 4 nm diameter sphere (the main peak of the distribution function); and cubic shapes containing $5 \times 5 \times 5$, $6 \times 6 \times 6$, $7 \times 7 \times 7$ and $8 \times 8 \times 8$ unit cells of silver crystallites, with edge lengths of 2.04 nm, 2.45 nm, 2.86 nm and 3.27 nm, respectively. These curves were obtained using the BODIES program from the ATSAS package

Table S1. χ^2 values for SAXS data plotted in Fig. 4

time, hours	χ^2
1	1.2
1.5	1.03
2	1.06
2.5	1.19
3	1.08
3.5	1.18
4	1.36
4.5	1.41
5	1.67
5.5	1.7
6	1.65
24	1.94
168	2.02

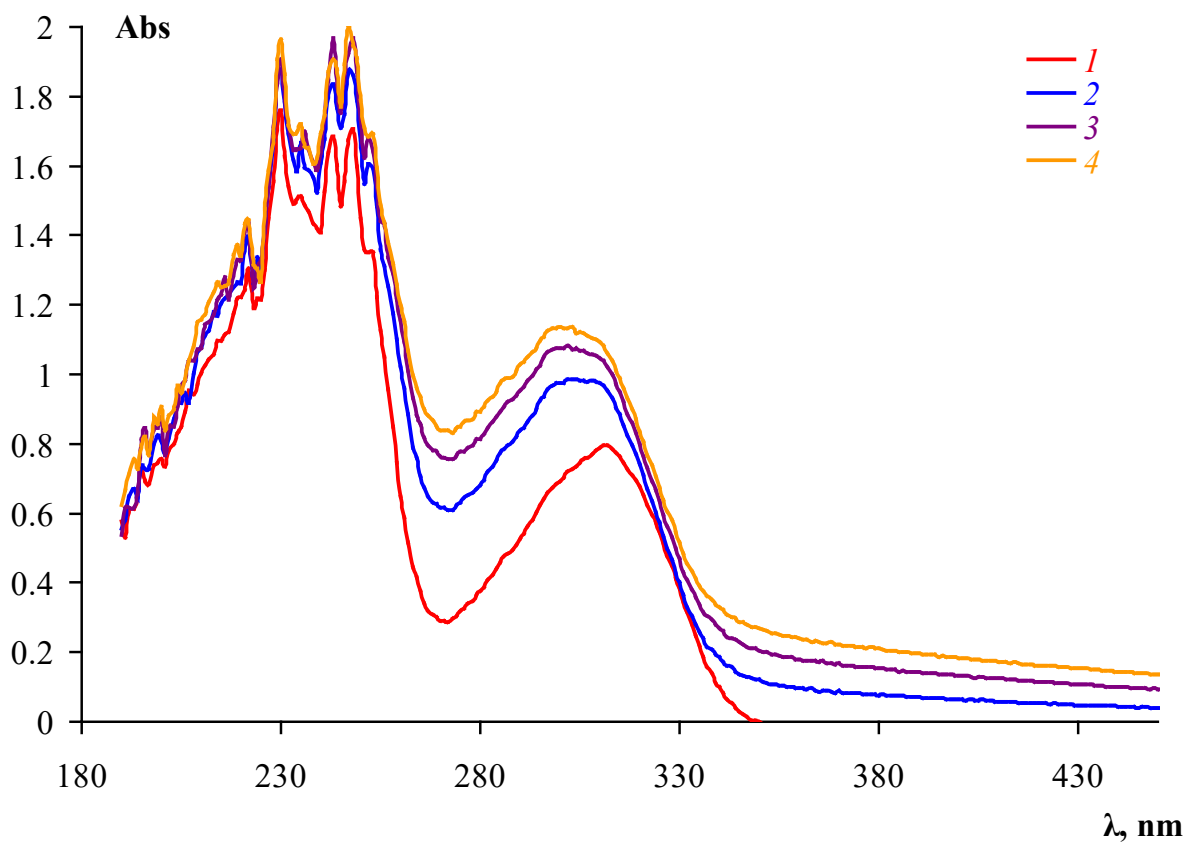


Figure S9. UV-vis spectra of a 2.9 g silver nitrate/ 100 g acetonitrile solution with the addition of 25 wt.% water NH_4OH in volumes of 0 (*1*), 200 (*2*), 300 (*3*) and 400 μl (*4*)